

LAST COPY
DO NOT REMOVE FROM FILE

UMBC #72-14

UR #416

#252

CONF-73-153-E

000 3065 33

C73/01/29

E-0252

(Unpublished)

Evidence for a Diffractive Component in Multiparticle Production
at 102 GeV.*

Rochester-Michigan Collaboration

C. M. Bromberg, D. Cohen, T. Ferbel[†], P. Slattery

University of Rochester

Rochester, New York 14627

and

J. W. Chapman, N. Green, B. P. Roe, A. A. Seidl[‡]

J. C. Vander Velde

University of Michigan

Ann Arbor, Michigan 48104

We have obtained an estimate of the inelastic diffractive cross section by measuring the spectrum of slow recoil protons coming from interactions of 102 GeV protons in hydrogen. The data are from a preliminary 5000 picture exposure of the NAL 30-inch bubble chamber. We find a value for the total cross section for single diffractive dissociation of 6.8 ± 1.0 mb, mainly contributed by the two-pronged and four-pronged topologies.

*Research supported by the U. S. Atomic Energy Commission.

[†]A. P. Sloan Research Fellow.

[‡]Contributed paper, Amer. Phys. Society, New York (January, 1973.)

The idea that high energy multiparticle production in hadron-hadron collisions may occur through two distinct components is not new.⁽¹⁾ It has been suggested that there may be a diffractive dissociation (D) component and a non-diffractive (ND) component, each of which have different multiplicity distributions and energy dependencies. Recently, multiplicity distributions obtained in pp collisions in the 13-200 GeV region have been used to estimate the ratio of the D to ND components; these estimates yield values for σ_D in the 7-9 mb range.⁽²⁾

In order to get a direct measure of a possible D component in pp collisions, we have analyzed the spectrum of slow protons produced in 102 GeV pp collisions in the NAL 30-inch hydrogen bubble chamber. The present data are from a preliminary 5000 picture exposure which yielded about 30 events/mb. We are studying the reaction

$$p + p \rightarrow p + \text{anything} \quad (1)$$

and we select events which have a proton with lab momentum less than 1.2 GeV/c. Such protons can be reliably identified by ionization and we will refer to them as slow protons. The mass (M) of the "anything" system can be obtained from a measurement of the momentum and angle of the slow proton, yielding a resolution in M^2 of $\pm .7 \text{ GeV}^2$. Our separation of elastic and inelastic events has been described elsewhere.⁽³⁾ Due to the rapid fall-off in transverse momentum, our lab momentum cut does not introduce any appreciable bias in the data for values of $M^2 < 80 \text{ GeV}^2$.

In what follows we will be mainly concerned with the type of diffractive process wherein only one of the incident protons dissociates. D-type events of this variety are expected to produce a peak at low M when the beam proton dissociates, and a high M continuum when the target proton dissociates. ND-type events (as well as the smaller DD-component which involves the simultaneous dissociation of both incident protons) will also contribute to the high M continuum. We look for evidence for such possible behavior by plotting the distribution in M^2 for various topologies in Figure 1. The data show a marked change in the slow proton spectrum as a function of the number of charged prongs (n). Diffractive peaks at low M^2 are clearly evident for the 2 and 4 prong topologies, but not for $n \geq 6$.

In Figure 2 we show the fraction of each topology that has both a slow proton and $M^2 < 50 \text{ GeV}^2$. (We multiply the observed fraction by two because of the symmetry of the pp system.) If we interpret the cross section for $M^2 < 50$ as having mainly a diffractive origin, then we conclude from this graph that 2-prong events may be almost totally diffractive whereas for events with $n \geq 6$, the diffractive component is no more than 10-20% of each topology. It is clear that the position of the cut on M^2 cannot critically alter the general features observed in Figure 2. (4)

In Figure 3a, we show $d\sigma/dM^2$ for all slow protons, integrated over transverse momentum up to $P_T^2 = .6 \text{ (GeV/c)}^2$. Figure 3b shows the distribution in M^2 of the average prong number associated

with any M^2 . A priori one expects $\langle n \rangle$ to increase with M^2 for events in which the beam proton dissociates. For target proton dissociation and ND events one expects a weaker correlation in the high M region. We note a definite break in the $\langle n \rangle$ data near $M^2 = 25 \text{ GeV}^2$, which we employ as an arbitrary cut-off value for the definition of the singly diffracted inelastic component in the data.

The cross section for $M^2 < 25 \text{ GeV}^2$ is $(3.4 \pm 0.5) \text{ mb}$ which yields a total single diffractive cross section of $2 \times (3.4 \pm 0.5) = (6.8 \pm 1.0) \text{ mb}$.⁽⁵⁾ This is in good agreement with the estimates of reference 2, and lends support to the idea of distinguishable and approximately constant values of σ_D and σ_{ND} at higher energies. If we set $\sigma_D = (6.8 \pm 1.0) \text{ mb}$, then we get $\sigma_{ND} = \sigma_{\text{inelastic}} - \sigma_D = (26.0 \pm 1.4) \text{ mb}$ at our energy. This is neglecting any possible double diffraction dissociation component σ_{DD} . Assuming factorization of vertices we can estimate $\sigma_{DD} = \sigma_D^2 / 4\sigma_{\text{elastic}}$ to be $\approx 1.7 \text{ mb}$. This value for σ_{DD} may be an overestimate because of the expected kinematic damping of this process (t_{min} effect). We nevertheless assign a value of $1.7 \pm 1 \text{ mb}$ to σ_{DD} . The total diffractive component is therefore estimated to be $8.5 \pm 1.5 \text{ mb}$.

Ignoring the small DD contribution, we obtain $\langle n_D \rangle = 3.44 \pm 0.17$ and $\langle n_{ND} \rangle = 7.20 \pm 0.21$ for the average multiplicity of these two components. We have examined the data for a possible difference in the P_1 behavior of slow protons from the D ($M^2 < 25 \text{ GeV}^2$) and ND ($25 < M^2 < 80 \text{ GeV}^2$) samples but find no significant difference. For $P_1^2 < .6 \text{ (GeV/c)}^2$ we find $\langle P_1^2 \rangle = (0.137 \pm 0.012) \text{ (GeV/c)}^2$ and $\langle P_1^2 \rangle_{ND} = (0.136 \pm 0.011) \text{ (GeV/c)}^2$. In Figure 4 we show the separate multiplicity distributions for the D and ND components in our data. We obtain $\langle n \rangle = 2.59 \pm 0.11$ and $D_-^2 = \langle n_-^2 \rangle - \langle n_- \rangle^2 =$

2.27 ± 0.19 for the ND component alone (where n_- is the number of negative tracks). We note that the ND component gives an excellent fit to a Poisson distribution in n_- . The χ^2 for the Poisson fit is 2.5 for 7 degrees of freedom. (6)

In summary, we have obtained an estimate of the diffractive production cross section in pp collisions at 102 GeV. Our value of 8.5 ± 1.5 mb for this inelastic component is consistent with recent estimates based on the assumption of two-component multiplicity distributions in high energy collisions (2). We wish to emphasize that our result is dependent on the identification of the observed low-mass enhancement in reaction (1) with the cross section for single-proton dissociation. Although other definitions for the singly-diffracted component are certainly possible, (7) we regard our identification of the peak at small-M values with σ_D as the simplest interpretation.

We thank the staff of National Accelerator Laboratory, and in particular that of the neutrino laboratory, for their help in obtaining the exposure. An illuminating discussion with G. L. Kane is appreciated.

References

1. K. G. Wilson, Cornell Preprint CLNS-3 (1970).
2. K. Fialkowski, Phys. Lett. 41B, 379 (1972); K. Fialkowski and M. Miettinen, RHEL report RPP/T/37 (1972); W. R. Frazer, R. D. Peccei, S. S. Pinsky, and C. Tan, University of California, San Diego, Preprint UCSD-10P10-113 (1972); C. Quigg and J. D. Jackson, NAL THY-93 (1972); L. Van Hove, CERN TH. 1581 (1972).

3. J. W. Chapman et al., Phys. Rev. Lett. 29, 1688 (1972).
4. We point out that the cut at $M^2 = 50 \text{ GeV}^2$ is generous since it allows 1 GeV for each charged track in the dissociating system when $n = 8$. Most diffractive models assign smaller values than this.
5. With considerably more data one could hope to obtain a more accurate measure of σ_D by taking into account its M dependence and making a background subtraction. Such refinements are not warranted at the present level of statistics.
6. This is not very surprising in view of the fact that the shape of the full sample of data does not differ markedly from a Poisson distribution at this energy (see ref. 3). It is of interest to look for similar behavior at higher energies where the full sample deviates more from Poisson.
7. Proponents of nova-type of models, in particular, would argue that our measurement of diffraction production may represent only a lower limit for the process. See for example the discussion of R. Slansky in the Yale Report No. 3075-18 (1972).

Figure Captions

Figure 1. The distribution of missing mass squared recoiling against the slow proton for various topologies. ($M^2 = 100 \text{ GeV}^2$ corresponds to $x = -.48$ in the c.m.) The division of events by prong number in the lowest graph is as follows: 8 prongs (38), 10 prongs (13), 12 prongs (9), 14 prongs (3). We estimate a 5 to 15% loss of events at high P_{\perp} in the region $80 < M^2 < 100$ due to our slow proton cut.

Figure 2. The fraction (times two) of each total topology having a slow proton with lab momentum less than 1.2 GeV/c and $M^2 < 50 \text{ GeV}^2$.

Figure 3. (a) The cross section $d\sigma/dM^2$ for all slow proton events with $P_1^2 < .6 (\text{GeV}/c)^2$. The values here have not been multiplied by the factor of two for symmetry. (b) The average prong number vs. M^2 for the same sample as (a).

Figure 4. Separate multiplicity distributions for D and ND components. The D component is comprised of twice the number of events with a slow proton and $M^2 < 25 \text{ GeV}^2$. The ND component is defined as the remainder of the inelastic events. The curve is a Poisson with $\langle n \rangle = 2.50$

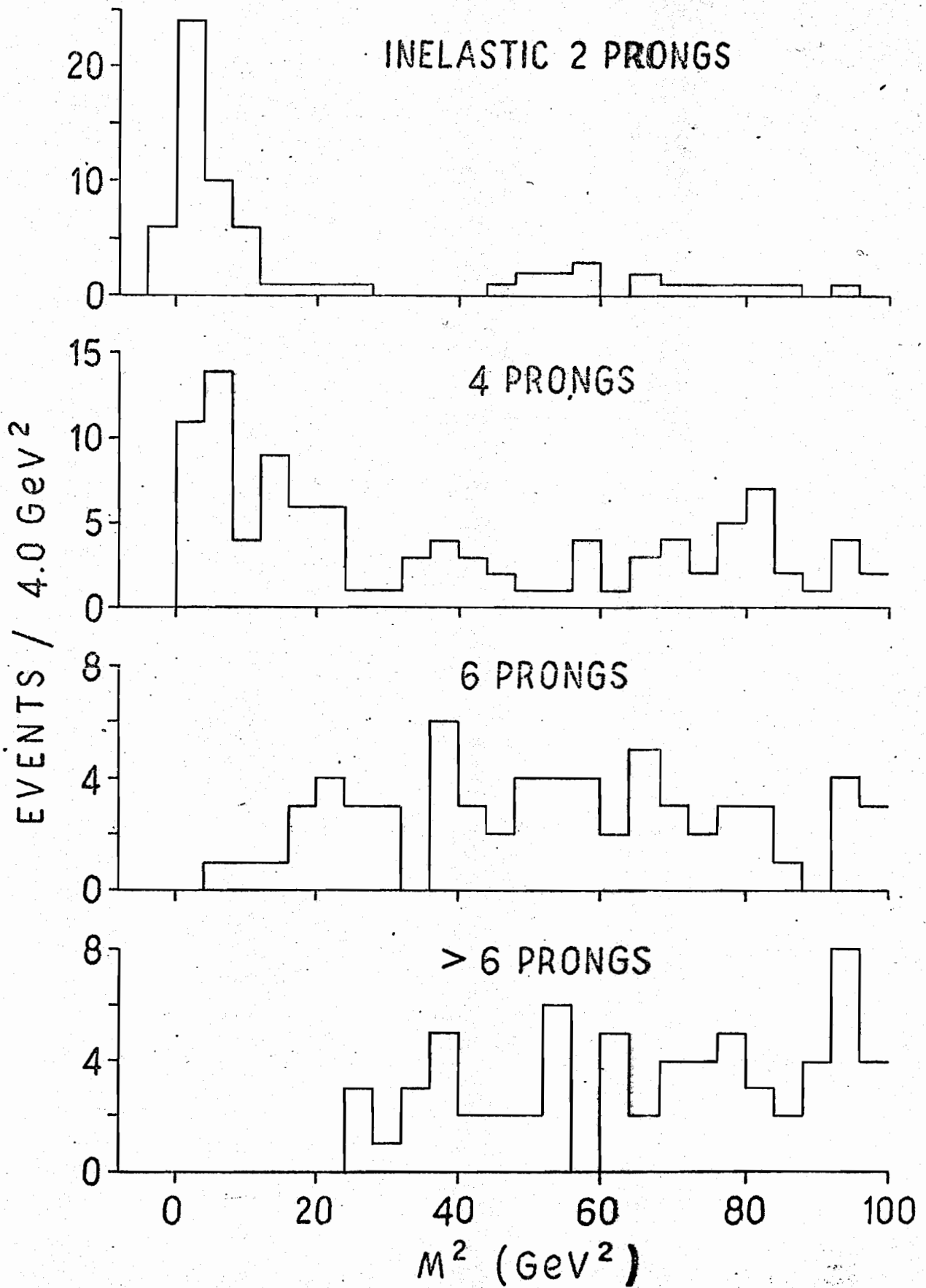


Figure 1

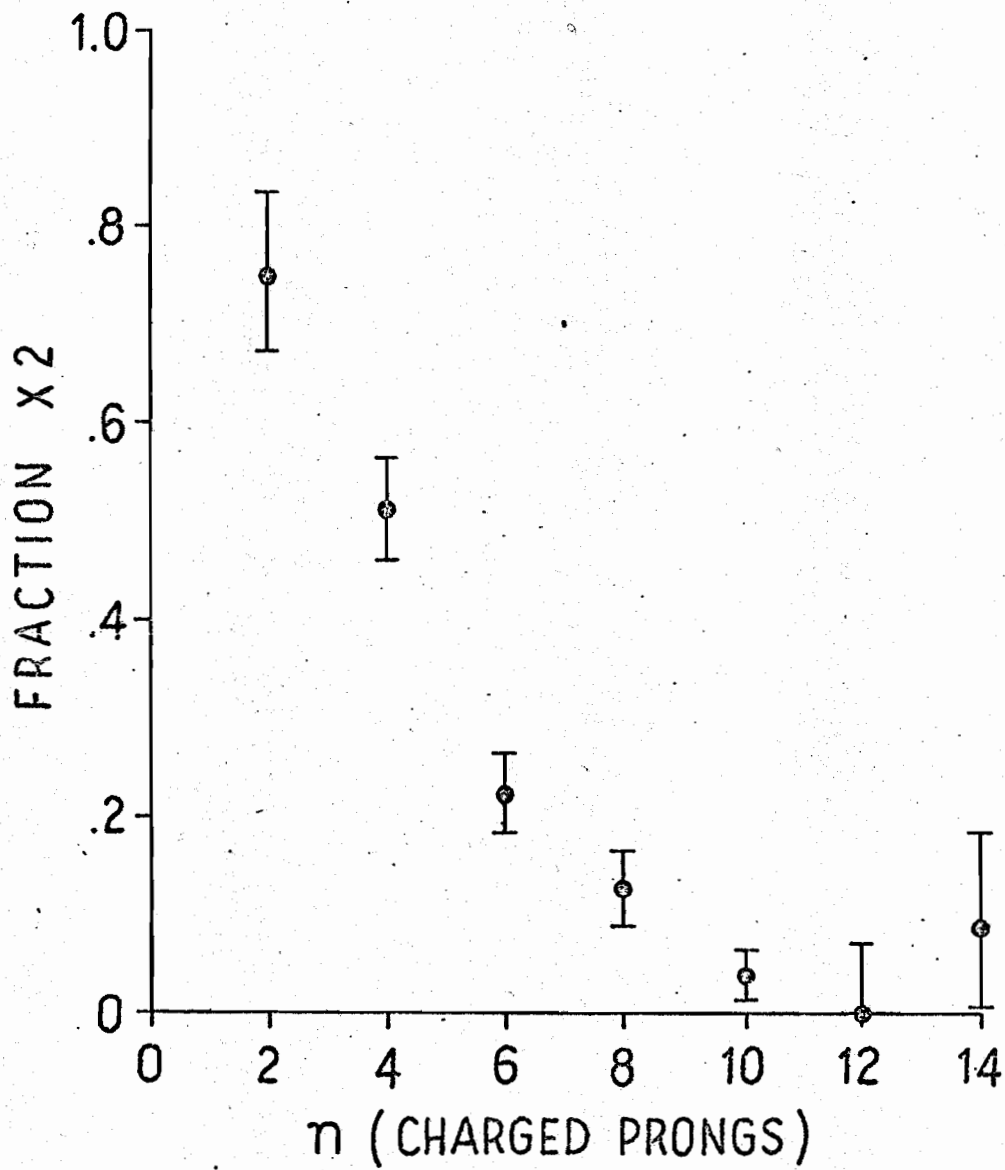


Figure 2

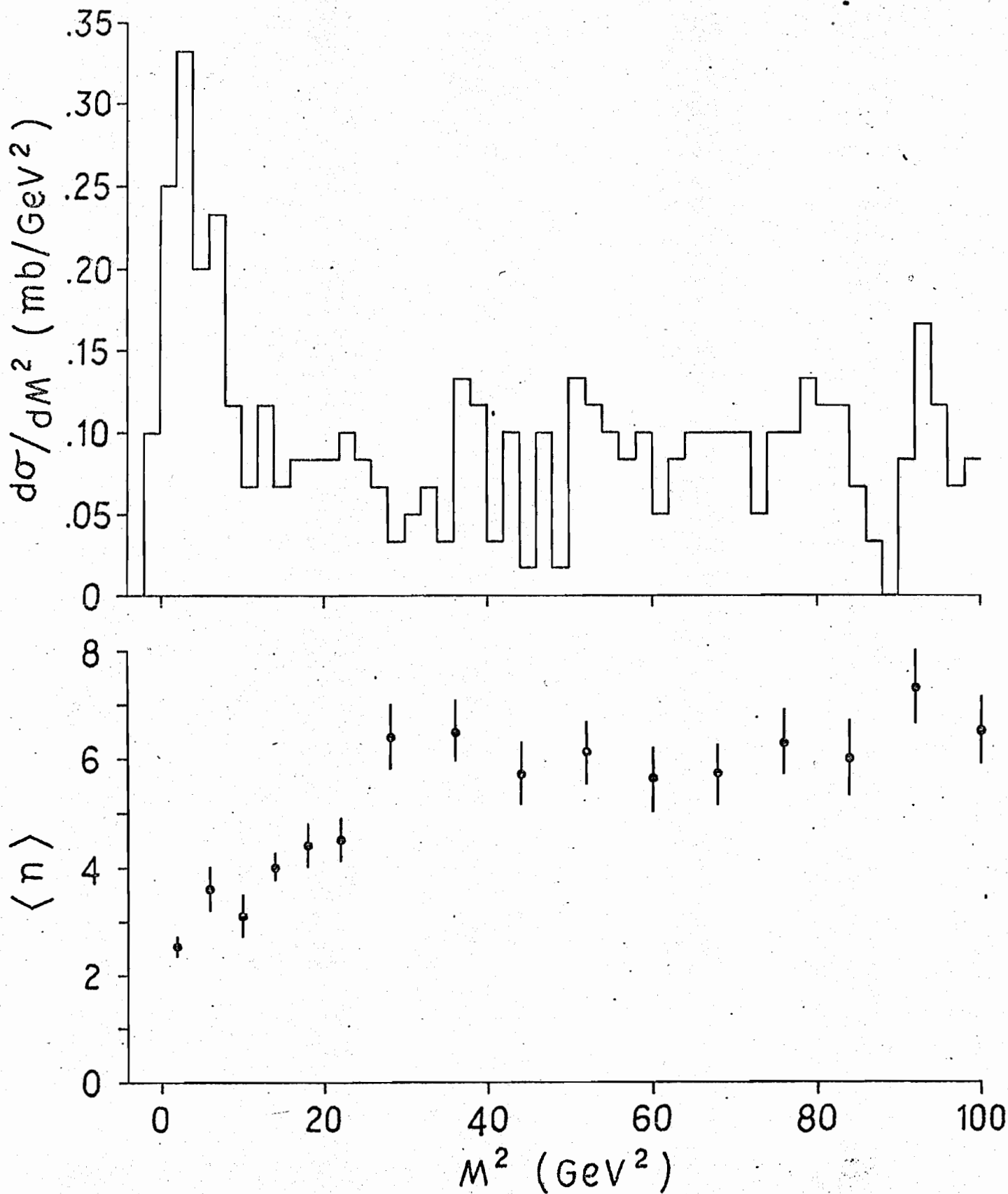


Figure 3

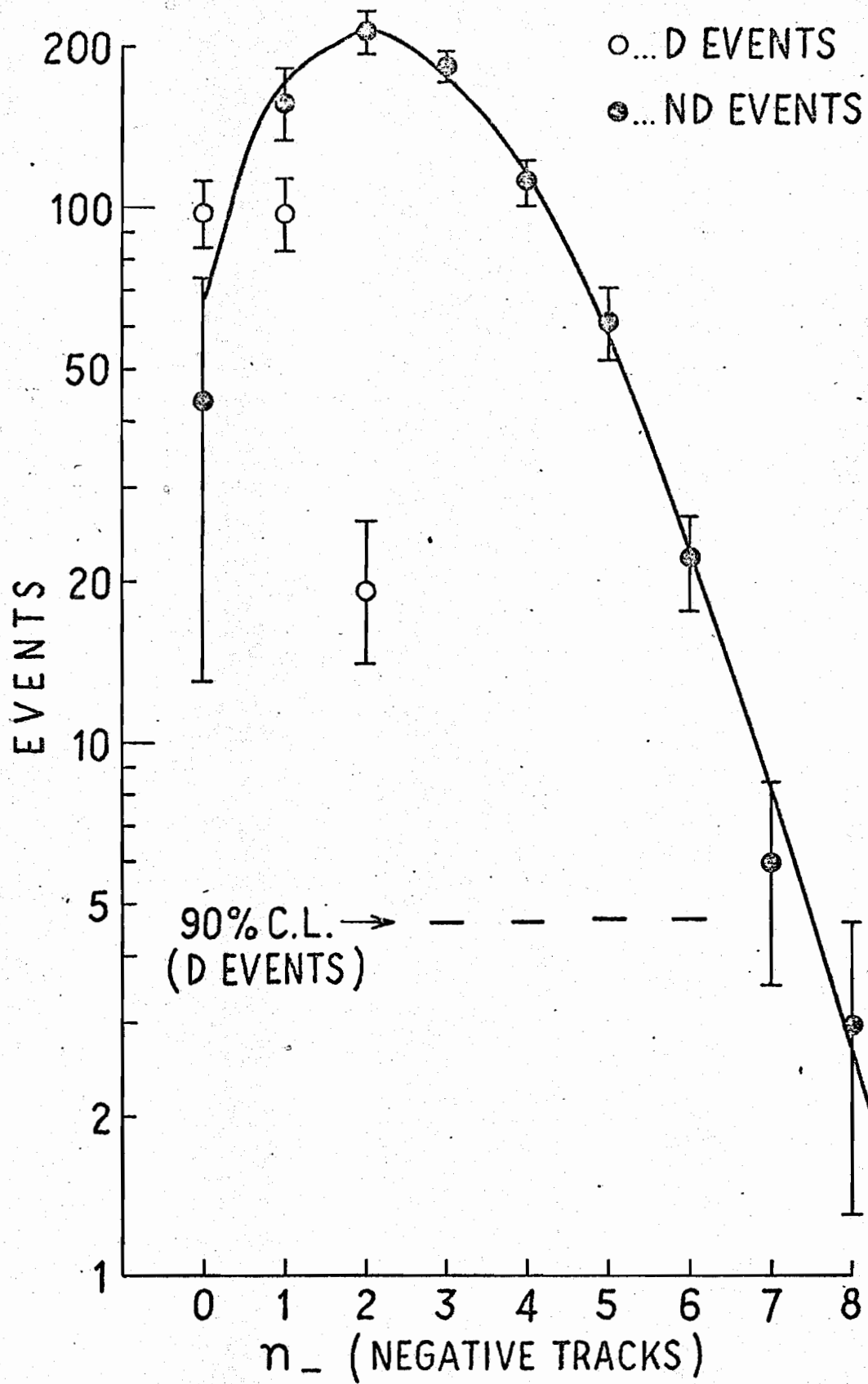


Figure 4